Pair excitations in solids

Gyeong-il Kweon
Department of Physics, Brown University, Providence, Rhode Island 02912

N. M. Lawandy
Department of Physics and Division of Engineering, Brown University, Providence, Rhode Island 02912
(Received 20 August 1993)

The pair-excitation probability in the weak-field regime is calculated using a fully quantized interaction Hamiltonian, for both the rotating- and fixed-atom cases. The peak of the absorption occurs at the sum of the final-state energies of the two atoms and the transition probability is shown to be proportional to the inverse square of the laser detuning and to the inverse cube of the nearest-neighbor distance. In addition, retardation effects result in a system size dependence for the transition rate not previously predicted. The significance of retardation effects is shown to depend on the excited-state coherence lifetime, the distance of closest approach, and the wavelength of the transition.

I. INTRODUCTION

Mixtures of several substances sometimes exhibit absorption or emission bands which neither of the basic constituents possesses. These absorption or emission bands correspond to the sum of the transition frequencies of two of the constituents. This phenomenon has been referred to as a double transition, simultaneous transition, or pair excitation, and has been known for some time. The first observation by Crawford and Welsh[1] in 1949 involved the vibrational absorption spectra of compressed H_2, O_2, and N_2 gases. Although the dipolar infrared absorption spectrum of homonuclear diatomic molecules is forbidden because of symmetry considerations, in the compressed state, the dipole selection rule may be broken by the polarization of one molecule by the quadrupole field of the other and/or by an asymmetric distortion of the electronic-wave-function distribution due to the overlapping of atomic orbitals during the collision.[2] In later studies, stronger lines were observed in mixtures of CO_2 and N_2, O_2 and H_2 (Refs. 3 and 4) and simultaneous rotational-vibrational transitions were measured in CO and H_2 mixtures.[5] In addition, simultaneous transitions in liquid mixtures[6,7] and solids[8-11] have been reported. Theoretical efforts,[12-17] along with a review article,[18] exist on the earlier observations of this phenomenon.

Other more refined gas-phase experiments were initiated by Gudzenko and Yakovlenko.[19,20] In the experiments[21] by White *et al.* on metal vapors, the authors observed the following processes using a white light source:

$$\mathrm{Ba}(6s^2\,{}^1S_0)+\mathrm{Ba}(6s^2\,{}^1S_0)+\hbar\omega(3394\ \text{Å}) \rightarrow \mathrm{Ba}(6p\,{}^1P_1^0)+\mathrm{Ba}(5d\,{}^1D_2)\ ,$$

$$\mathrm{Ba}(6s^2\,{}^1S_0)+\mathrm{Tl}(6p\,{}^2P_{1/2}^0)+\hbar\omega(3867\ \text{Å}) \rightarrow \mathrm{Ba}(6p\,{}^1P_1^0)+\mathrm{Tl}(6p\,{}^2P_{3/2}^0)\ .$$

Using a laser source, they also observed the reverse of the former process.[22] Pair excitation has been reported for intermediate states lying in the continuum,[23] for dipole-quadrupole collisions,[24] and for two-photon absorption.[25] A review article on laser-induced collision processes where pair excitation is considered as one special case also exists.[26]

Pair excitation has also been observed many years ago in various crystalline solids such as solid hydrogen,[8] $PrCl_3$,[9] Pr:$LaCl_3$,[27] and PrF_3,[28] and its reverse process has been observed in $YbPO_4$.[29] Cross-section ratios comparing pair absorption to single-ion transition have been measured for the above systems. These will be discussed in a separate section of the paper, where we will directly apply the theory developed for both transition rates as well as polarization dependence. More recently there has been a vigorous effort in quantum electronics devoted to the phenomenon of photon avalanche.[30] This intriguing effect has attracted much attention because of its highly nonlinear thresholdlike behavior as well as its potential applications for frequency upconversion.[31] Although the mechanism by which the initial population of the excited states is achieved is still being debated, one potential candidate is pair absorption or cluster absorption. In this context, the present work may provide a framework for accurately calculating the avalanche initiation process as well as shed light on the role of cluster-size dependence on the rate.

Most of the earlier theories for this phenomenon either have neglected the importance of the intermediate states or are based on the impact theory, where the colliding atomic pairs are assumed to follow a straight trajectory. The impact theory is probably the most suitable way to analyze the later series of experiments, where the temperature of the gas is high and pressure is on the order of a few torr. However, the long-range nature of the interaction process, which is mediated by a potential varying as the inverse cube of the separation, makes the validity of such an approach questionable at high pressures[2,21] and/or low temperatures.[8] The impact models which are not fully quantized are less suited to the study of nearly static systems such as liquid mixtures[6,7] and solids,[8-11]

where the fixed positions allow significant retardation effects to manifest themselves.

In this article, we solve this old problem for the static-atom limit in solids using a fully retarded formulation. The electromagnetic field as well as the atoms are fully quantized, and time-dependent third-order perturbation theory is used. The atoms or molecules are assumed fixed in space, so the theory will best describe the pair excitation in solids, such as ion pairs in crystals. In the case of gas mixtures, Harris and White[32] pointed out that, although dipole-dipole interactions are stronger at closer distances, the relative atomic velocity is high and the collision duration is short. This results in a contribution to the pair excitation which is maximized at some separation and is not a monotonically decreasing function of distance. To account for the relative motions of the atoms, a radial distribution function may be introduced as a weighting factor.[2] In addition, the model we present neglects three-body collisions or higher-order processes, since two-body coupling accounts for most of the transition. Earlier papers on high gas pressures or on liquids and solids have confirmed that, even at very high densities, the transition rate is still proportional to the square of the density or product of two species densities, confirming that two-body interactions are dominant.

In order to elucidate more clearly the salient features of this theory, the analysis will be confined to the pair-excitation process where all the real and virtual transitions are dipole allowed. In most of the earlier treatments, the orientation of the dipole-transition-moment vectors was constrained in order to simplify the problem. Often the quantization axis was taken as the line joining the two particles with magnetic quantum number zero, while others considered the case where the quantization axis is fixed in space. In this article, we will consider the more general latter case in various limits, including the case of freely rotating atoms.

Figure 1 shows the relevant energy-level diagrams involved in calculating the required matrix elements. $|o\rangle$ and $|o'\rangle$ are the ground states of atoms A and B, $|p\rangle$ and $|m\rangle$ are the final states, and $|r\rangle$ is the intermediate state of atom A. Figure 2 shows the relevant Feynman diagrams in the process. These diagrams are very similar to those required to treat the problem of circular dichroism arising from the coupling between nonidentical chromophores,[33] and can also be used for the calculation of laser-induced collisional energy transfer. In the collisional-energy-transfer case, state $|o\rangle$ is the excited state and $|p\rangle$ is the ground state.

II. EVALUATION OF THE TRANSITION RATE

The required transition matrix elements in third-order perturbation theory in the multipolar interaction Hamiltonian are given by

$$M_{fi}=\sum_{\mathrm{I,II}}\frac{\langle f|-(1/\varepsilon_0)\boldsymbol{\mu}\cdot\mathbf{d}^{\perp}|\mathrm{II}\rangle\langle\mathrm{II}|-(1/\varepsilon_0)\boldsymbol{\mu}\cdot\mathbf{d}^{\perp}|\mathrm{I}\rangle\langle\mathrm{I}|-(1/\varepsilon_0)\boldsymbol{\mu}\cdot\mathbf{d}^{\perp}|i\rangle}{E_{i\mathrm{I}}E_{i\mathrm{II}}}\ , \tag{1}$$

where $|i\rangle$, $|\mathrm{I}\rangle$, $|\mathrm{II}\rangle$, and $|f\rangle$ are the initial, first intermediate, second intermediate, and final states of the total system, $\boldsymbol{\mu}$ is the electric-dipole-moment operator, $\mathbf{d}$ is the microscopic displacement vector, and $E_{i\mathrm{I}}$ is the energy difference between the states $|i\rangle$ and $|\mathrm{I}\rangle$. The microscopic displacement vector is given as follows:

$$\mathbf{d}^{\perp}(\mathbf{r})=i\sum_{\mathbf{k},\lambda}\left[\frac{\hbar ck\varepsilon_0}{2V}\right]^{1/2}\times\{e^{(\lambda)}(\mathbf{k})a^{(\lambda)}(\mathbf{k})e^{i\mathbf{k}\cdot\mathbf{r}}-\bar{e}^{(\lambda)}(\mathbf{k})a^{\dagger(\lambda)}(\mathbf{k})e^{-i\mathbf{k}\cdot\mathbf{r}}\}\ , \tag{2}$$

where $\mathbf{k}$ is the virtual photon wave vector, λ is the polarization index, $\mathbf{e}^{(\lambda)}(\mathbf{k})$ is the directional unit vector for the polarization of the electric field, $a^{(\lambda)}(\mathbf{k})$ is the field annihilation operator, $\bar{\mathbf{e}}^{(\lambda)}(\mathbf{k})$ and $a^{\dagger(\lambda)}(\mathbf{k})$ are the complex and Hermitian conjugates of $\mathbf{e}^{(\lambda)}(\mathbf{k})$ and $a^{(\lambda)}(\mathbf{k})$, respectively, and V is the quantizing volume. As an example, for the first diagram in Fig. 2,

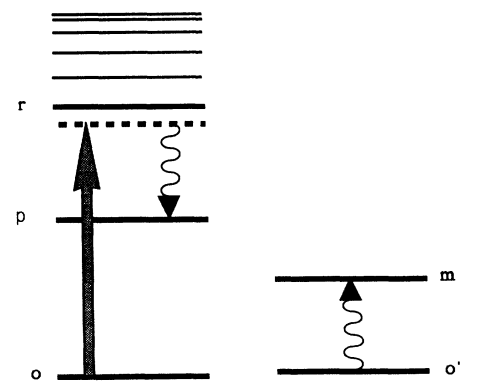

FIG. 1. Relevant energy levels for the pair-excitation process.

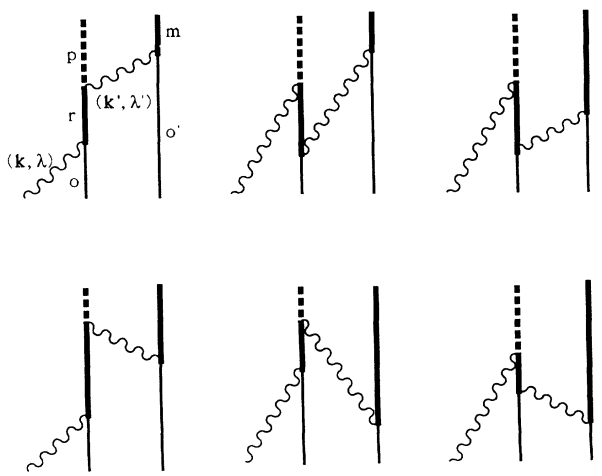

FIG. 2. Required Feynman diagrams for the process.

$$E_{iI}=E_o+E_{o'}+n\hbar\omega-\{E_r+E_{o'}+(n-1)\hbar\omega\}$$

$$=E_{or}+\hbar\omega$$

and likewise

$$E_{iII}=E_{op}+\hbar\omega-\hbar\omega' .$$

Using this result, the contribution to the transition matrix from the first diagram is found to be

$$M_1=-i\mu_i^{mo'}\left[\frac{\hbar c}{2\varepsilon_0 V}\right]^{3/2}(nkk'^2)^{1/2}\times e^{i\mathbf{k}'\cdot(\mathbf{r}_B-\mathbf{r}_A)}e^{i\mathbf{k}\cdot\mathbf{r}_A}\mathbf{e}_i^{(\lambda')}(\mathbf{k}')\times\bar{\mathbf{e}}_j^{(\lambda')}(\mathbf{k}')e_k^{(\lambda)}(\mathbf{k})\sum_r\frac{\mu_j^{pr}\mu_k^{ro}}{(E_{ro}-\hbar\omega)(E_{po}-\hbar\omega+\hbar\omega')} . \tag{3}$$

When contributions from all other five diagrams are added together, we arrive at the total transition matrix given below:

$$\begin{aligned}M&=\sum_{i=1}^{6}M_i\\&=-i\sum_{\mathbf{k}',\lambda'}\left[\frac{\hbar c}{2\varepsilon_0 V}\right]^{3/2}(nkk'^2)^{1/2}e^{i\mathbf{k}\cdot\mathbf{r}_A}\mathbf{e}_i^{(\lambda')}(\mathbf{k}')\bar{e}_j^{(\lambda')}(\mathbf{k}')e_k^{(\lambda)}(\mathbf{k})\\&\quad\times\left[e^{i\mathbf{k}'\cdot(\mathbf{r}_B-\mathbf{r}_A)}\left\{\sum_r\frac{\mu_i^{mo'}\mu_j^{pr}\mu_k^{ro}}{(E_{ro}-\hbar\omega)(E_{po}-\hbar\omega+\hbar\omega')}+\sum_r\frac{\mu_i^{mo'}\mu_j^{ro}\mu_k^{pr}}{(E_{ro}+\hbar\omega')(E_{po}-\hbar\omega+\hbar\omega')}+\sum_r\frac{\mu_i^{mo'}\mu_j^{ro}\mu_k^{pr}}{(E_{ro}+\hbar\omega')(E_{ro}+E_{mo'})}\right\}\right.\\&\quad\left.+e^{-i\mathbf{k}'\cdot(\mathbf{r}_B-\mathbf{r}_A)}\left\{\sum_r\frac{\mu_i^{pr}\mu_j^{mo'}\mu_k^{ro}}{(E_{ro}-\hbar\omega)(E_{ro}+E_{mo'}-\hbar\omega+\hbar\omega')}+\sum_r\frac{\mu_i^{pr}\mu_j^{mo'}\mu_k^{ro}}{(E_{mo'}+\hbar\omega')(E_{ro}+E_{mo'}-\hbar\omega+\hbar\omega')}+\sum_r\frac{\mu_i^{ro}\mu_j^{mo'}\mu_k^{pr}}{(E_{mo'}+\hbar\omega')(E_{ro}+E_{mo'})}\right\}\right] .\end{aligned} \tag{4}$$

The above Eq. (4) can be simplified using the energy conservation condition, $E_i\equiv E_o+E_{o'}+n\hbar\omega=E_f\equiv E_p+E_m+(n-1)\hbar\omega$, i.e., $E_{po}+E_{mo'}=\hbar\omega$, and remembering that we are dealing with the pair-excitation process, we restrict ourselves to the case where $E_p>E_o$ and $E_m>E_{o'}$, i.e., $E_{po}>0$ and $E_{mo'}>0$. We define $\mathbf{R}\equiv\mathbf{r}_B-\mathbf{r}_A$, and the following identity from complex-variable theory can be used to further simplify this result:

$$\frac{p}{x}\frac{p}{y}=\frac{p}{x}\frac{p}{x+y}+\frac{p}{y}\frac{p}{x+y}-\pi^2\delta(x)\delta(y) , \tag{5}$$

where p stands for a Cauchy principal value and x and y are mathematical expressions containing simple poles. The second term in the first curly bracket in Eq. (4) becomes

$$\begin{aligned}\frac{1}{(E_{ro}+\hbar\omega')(E_{po}-\hbar\omega+\hbar\omega')}&=\frac{-1}{(E_{ro}+\hbar\omega')(E_{ro}-E_{po}+\hbar\omega)}+\frac{1}{(E_{po}-\hbar\omega+\hbar\omega')(E_{ro}-E_{po}+\hbar\omega)}\\&\quad+\pi^2\delta(E_{ro}+\hbar\omega')\delta(E_{po}-\hbar\omega+\hbar\omega')\\&=\frac{-1}{(E_{ro}+\hbar\omega')(\hbar\omega-E_{pr})}+\frac{1}{(\hbar\omega'-E_{mo'})(\hbar\omega-E_{pr})}\\&\quad+\pi^2\delta(E_{ro}+\hbar\omega')\delta(\hbar\omega'-E_{mo'}) ,\end{aligned} \tag{6}$$

where the energy-conservation condition has been used in the last step. With this simplification, the expression in the curly bracket is given by

$$\begin{aligned}\{\cdots\}_{\mathrm{I}}=\mu_i^{mo'}\left[-\frac{1}{(\hbar\omega'-E_{mo'})}\sum_r\frac{\mu_j^{pr}\mu_k^{ro}}{(\hbar\omega-E_{ro})}-\sum_r\frac{\mu_j^{ro}\mu_k^{pr}}{(E_{ro}+\hbar\omega')(\hbar\omega-E_{pr})}+\frac{1}{(\hbar\omega'-E_{mo'})}\sum_r\frac{\mu_j^{ro}\mu_k^{pr}}{(\hbar\omega-E_{pr})}\right.\\\left.+\pi^2\delta(\hbar\omega'-E_{mo'})\sum_r\mu_j^{ro}\mu_k^{pr}\delta(\hbar\omega'+E_{ro})+\sum_r\frac{\mu_j^{ro}\mu_k^{pr}}{(E_{ro}+\hbar\omega')(E_{ro}+E_{mo'})}\right] .\end{aligned} \tag{7}$$

Combining the second and fifth terms in Eq. (7) yields

$$\frac{1}{E_{ro}+E_{mo'}}-\frac{1}{\hbar\omega-E_{pr}}=\frac{\hbar\omega-E_{pr}-E_{ro}-E_{mo'}}{(E_{ro}+E_{mo'})(\hbar\omega-E_{pr})}=\frac{\hbar\omega-E_{po}-E_{mo'}}{(E_{ro}+E_{mo'})(\hbar\omega-E_{pr})}=\frac{0}{(E_{ro}+E_{mo'})(\hbar\omega-E_{pr})}=0\ , \tag{8}$$

where the last step follows from the energy-conservation condition. With Eq. (8) and some rearrangement, Eq. (7) becomes

$$\{\cdots\}_{\mathrm{I}}=-\mu_i^{mo'}\left[\frac{1}{(\hbar\omega'-E_{mo'})}\sum_r\left\{\frac{\mu_j^{pr}\mu_k^{ro}}{\hbar\omega-E_{ro}}-\frac{\mu_k^{pr}\mu_j^{ro}}{\hbar\omega-E_{pr}}\right\}-\pi^2\sum_r\mu_j^{ro}\mu_k^{pr}\delta_{E_{mo'}-E_{ro}}\right]\ . \tag{9}$$

With the help of Eq. (5), the second term in the second curly bracket in Eq. (4) becomes

$$\begin{aligned}\frac{1}{(E_{mo'}+\hbar\omega')(E_{ro}+E_{mo'}-\hbar\omega+\hbar\omega')}&=\frac{-1}{(E_{mo'}+\hbar\omega')(-E_{ro}+\hbar\omega)}-\frac{1}{(-E_{ro}-E_{mo'}+\hbar\omega-\hbar\omega')(-E_{ro}+\hbar\omega)}\\&\quad+\pi^2\delta(E_{mo'}+\hbar\omega')\delta(-E_{ro}-E_{mo'}+\hbar\omega-\hbar\omega')\\&=\frac{-1}{(\hbar\omega'+E_{mo'})(\hbar\omega-E_{ro})}+\frac{1}{(\hbar\omega'-E_{pr})(\hbar\omega-E_{ro})}\ ,\end{aligned} \tag{10}$$

where the delta function vanishes because of the initial assumption $E_{mo'}>0$. Equation (10) transforms the second curly bracket in Eq. (4) into

$$\begin{aligned}\{\cdots\}_{\mathrm{II}}=\mu_j^{mo'}\Bigg[&-\sum_r\frac{\mu_i^{pr}\mu_k^{ro}}{(\hbar\omega-E_{ro})(E_{ro}-E_{po}+\hbar\omega')}-\sum_r\frac{\mu_i^{pr}\mu_k^{ro}}{(\hbar\omega'+E_{mo'})(\hbar\omega-E_{ro})}\\&+\sum_r\frac{\mu_i^{pr}\mu_k^{ro}}{(\hbar\omega'-E_{pr})(\hbar\omega-E_{ro})}+\sum_r\frac{\mu_i^{ro}\mu_k^{pr}}{(\hbar\omega'+E_{mo'})(E_{ro}+E_{mo'})}\Bigg]\ .\end{aligned} \tag{11}$$

After some algebra, the first term in Eq. (11) can be shown to be the exact negative of the third term, resulting in

$$\{\cdots\}_{\mathrm{II}}=-\mu_j^{mo'}\frac{1}{(\hbar\omega'+E_{mo'})}\sum_r\left\{\frac{\mu_i^{pr}\mu_k^{ro}}{\hbar\omega-E_{ro}}-\frac{\mu_k^{pr}\mu_i^{ro}}{E_{ro}+E_{mo'}}\right\}\ . \tag{12}$$

Assuming no resonance between the intermediate states of atom A and final state of atom B, i.e., $\delta_{E_{mo'}-E_{ro}}=0$, the total matrix element further simplifies to the following expression:

$$\begin{aligned}M=i&\left[\frac{\hbar c}{2\varepsilon_0 V}\right]^{3/2}(nk)^{1/2}\mathbf{e}^{i\mathbf{k}\cdot\mathbf{r}_A}\mathbf{e}_k^{(\lambda)}(\mathbf{k})\\&\times\Bigg[\sum_r\left\{\frac{\mu_j^{pr}\mu_k^{ro}}{\hbar\omega-E_{ro}}-\frac{\mu_k^{pr}\mu_j^{ro}}{\hbar\omega-E_{pr}}\right\}\mu_i^{mo'}\sum_{\mathbf{k}',\lambda'}\mathbf{e}_i^{(\lambda')}(\mathbf{k}')\bar{\mathbf{e}}_j^{(\lambda')}(\mathbf{k}')\frac{k'}{\hbar\omega'-E_{mo'}}e^{i\mathbf{k}'\cdot\mathbf{R}}\\&+\sum_r\left\{\frac{\mu_i^{pr}\mu_k^{ro}}{\hbar\omega-E_{ro}}-\frac{\mu_k^{pr}\mu_i^{ro}}{E_{ro}+E_{mo'}}\right\}\mu_j^{mo'}\sum_{\mathbf{k}',\lambda'}\mathbf{e}_i^{(\lambda')}(\mathbf{k}')\bar{\mathbf{e}}_j^{(\lambda')}(\mathbf{k}')\frac{k'}{\hbar\omega'+E_{mo'}}e^{-i\mathbf{k}'\cdot\mathbf{R}}\Bigg]\ .\end{aligned} \tag{13}$$

The property of the photon polarization is

$$\sum_{\lambda'}\mathbf{e}_i^{(\lambda')}(\mathbf{k}')\bar{\mathbf{e}}_j^{(\lambda')}(\mathbf{k}')=(\delta_{ij}-\hat{k}_i'\hat{k}_j')\ , \tag{14}$$

and the summation over the photon wave vectors can be transformed into an integral in the limit of a large quantizing volume.

$$\frac{1}{V}\sum_{\mathbf{k}'}=\int\frac{d^3k'}{(2\pi)^3}\ . \tag{15}$$

Defining $k_o\equiv E_{mo'}/\hbar c$, this integral can be cast in the following form:

$$\int\frac{d^3k'}{(2\pi)^3}(\delta_{ij}-\hat{k}_i'\hat{k}_j')e^{\pm i\mathbf{k}'\cdot\mathbf{R}}=\frac{1}{2\pi^2}\int k'^2dk'\tau_{ij}(k'R)\ , \tag{16}$$

where

$$\begin{aligned}\tau_{ij}(k'R)&=\tau_{ji}(k'R)\\&=(\delta_{ij}-\hat{R}_i\hat{R}_j)\frac{\sin(k'R)}{(k'R)}\\&\quad+(\delta_{ij}-3\hat{R}_i\hat{R}_j)\left\{\frac{\cos(k'R)}{(k'R)^2}-\frac{\sin(k'R)}{(k'R)^3}\right\}\ .\end{aligned} \tag{17}$$

Further basic manipulation along with the energy-conservation equation results in

$$M=\frac{i}{\pi^2}\left[\frac{1}{2\varepsilon_0}\right]^{3/2}\left[\frac{n\hbar ck}{V}\right]^{1/2} e^{i\mathbf{k}\cdot\mathbf{r}_A}\mathbf{e}_k^{(\lambda)}(\mathbf{k})\mu_i^{mo'} \times\sum_r\left\{\frac{\mu_j^{pr}\mu_k^{ro}}{\hbar\omega-E_{ro}}-\frac{\mu_k^{pr}\mu_j^{ro}}{E_{ro}+E_{mo'}}\right\}\int dk'\frac{k'^4\tau_{ij}(k'R)}{k'^2-k_o^2} . \tag{18}$$

The integral appearing in Eq. (18) can be directly evaluated and yields the following results:

$$\int dk'\frac{k'^4\tau_{ij}(k'R)}{k'^2-k_o^2}=-\frac{\pi}{2R^3}V_{ij}(k_oR) , \tag{19}$$

where V_{ij} is defined as

$$V_{ij}(k_oR)\equiv(\delta_{ij}-3\hat{R}_i\hat{R}_j)\{\cos(k_oR)+(k_oR)\sin(k_oR)\} -(\delta_{ij}-\hat{R}_i\hat{R}_j)(k_oR)^2\cos(k_oR) . \tag{20}$$

Further defining a quantity somewhat similar to the conventional dynamic polarizability given by

$$\alpha_{jk}\equiv\sum_r\left\{\frac{\mu_j^{pr}\mu_k^{ro}}{\hbar\omega-E_{ro}}-\frac{\mu_k^{pr}\mu_j^{ro}}{E_{ro}+E_{mo'}}\right\} , \tag{21}$$

the transition matrix assumes the compact form

$$M=-\frac{i}{2\pi R^3}\left[\frac{1}{2\varepsilon_0}\right]^{3/2}\left[\frac{n\hbar ck}{V}\right]^{1/2} \times e^{i\mathbf{k}\cdot\mathbf{r}_A}\mathbf{e}_k^{(\lambda)}(\mathbf{k})\mu_i^{mo'}\alpha_{jk}V_{ij}(k_oR) . \tag{22}$$

Using the matrix element given in Eq. (22), the transition rate per unit volume per unit time is given by

$$d\Gamma=\frac{2\pi}{\hbar}N_AN_B|M_{fi}|^2\rho_f , \tag{23}$$

where N_A and N_B are the number densities of atoms A and B, respectively, and ρ_f is the density of final states. This results in:

$$d\Gamma=\frac{1}{16\pi\hbar\varepsilon_0^3R^6}N_AN_B\frac{n\hbar ck}{V}\mathbf{e}_k^{(\lambda)}(\mathbf{k})\bar{e}_n^{(\lambda)}(\mathbf{k}) \times\mu_i^{mo'}\bar{\mu}_l^{mo'}\alpha_{jk}\bar{\alpha}_{mn}V_{ij}(k_oR)\bar{V}_{lm}(k_oR)\rho_f . \tag{24}$$

The transition rate derived can be evaluated for several limits of transition-moment orientations. In the low-gas-density regime, especially for nonpolar gases, the transition dipoles will be freely rotating. In the case of crystals, the symmetry directions of the crystal can be used as a quantization axis. First, the freely rotating model is discussed, as it leads to a relatively simple expression for the transition rate. In this limit, the dipole moments of atoms A and B are independent, and the rotationally averaged transition rate becomes

$$\langle d\Gamma\rangle=\frac{1}{16\pi\hbar\varepsilon_0^3R^6}N_AN_B\frac{n\hbar ck}{V}\mathbf{e}_k^{(\lambda)}(\mathbf{k})\bar{\mathbf{e}}_n^{(\lambda)}(\mathbf{k}) \times\langle\mu_i^{mo'}\bar{\mu}_l^{mo'}\rangle\langle\alpha_{jk}\bar{\alpha}_{mn}\rangle V_{ij}(k_oR)\bar{V}_{lm}(k_oR)\rho_f , \tag{25}$$

where the $\langle\cdots\rangle$ stand for rotational averaging. Direct evaluation of the averaging gives

$$\langle\mu_i^{mo'}\bar{\mu}_l^{mo'}\rangle=\tfrac{1}{3}\delta_{il}|\mu^{mo'}|^2 \tag{26a}$$

and

$$\langle\alpha_{jk}\bar{\alpha}_{mn}\rangle=\tfrac{1}{30}[\delta_{jk}\delta_{mn}(4\delta_{\lambda\mu}\delta_{\nu\pi}-\delta_{\lambda\nu}\delta_{\mu\pi}-\delta_{\lambda\pi}\delta_{\mu\nu})+\delta_{jm}\delta_{kn}(-\delta_{\lambda\mu}\delta_{\nu\pi}+4\delta_{\lambda\nu}\delta_{\mu\pi}-\delta_{\lambda\pi}\delta_{\mu\nu}) +\delta_{jn}\delta_{km}(-\delta_{\lambda\mu}\delta_{\nu\pi}-\delta_{\lambda\nu}\delta_{\mu\pi}+4\delta_{\lambda\pi}\delta_{\mu\nu})]\alpha_{\lambda\mu}\bar{\alpha}_{\nu\pi} . \tag{26b}$$

The photon occupation numbers can be expressed in terms of an intensity given by

$$\mathrm{I}(\omega)=\frac{nc\hbar\omega}{V} . \tag{27}$$

Further assuming that the excitation source is linearly polarized and given as

$$\mathbf{e}_n^{(\lambda)}(\mathbf{k})\bar{\mathbf{e}}_n^{(\lambda)}(\mathbf{k})=1 \tag{28a}$$

and

$$\mathbf{e}_n^{(\lambda)}(\mathbf{k})\bar{\mathbf{e}}_k^{(\lambda)}(\mathbf{k})=\bar{\mathbf{e}}_n^{(\lambda)}(\mathbf{k})\mathbf{e}_k^{(\lambda)}(\mathbf{k})=\mathbf{e}_n^{(\lambda)}(\mathbf{k})\mathbf{e}_k^{(\lambda)}(\mathbf{k}) , \tag{28b}$$

with these assumptions the transition rate is simplified to

$$\langle d\Gamma\rangle=\frac{N_AN_BI(\omega)|\mu^{mo'}|^2}{1440\pi\varepsilon_0^3\hbar cR^6}\rho_f[\{(1+3|\mathbf{e}_k^{(\lambda)}\cdot\hat{R}|^2)V_1^2+(1-|\mathbf{e}_k^{(\lambda)}\cdot\hat{R}|^2)(V_2^2-2V_1V_2)\}(3\alpha_{\lambda\lambda}\bar{\alpha}_{\mu\mu}-2\alpha_{\lambda\mu}\bar{\alpha}_{\lambda\mu}+3\alpha_{\lambda\mu}\bar{\alpha}_{\mu\lambda}) +(6V_1^2-4V_1V_2+2V_2^2)(-\alpha_{\lambda\lambda}\bar{\alpha}_{\mu\mu}+4\alpha_{\lambda\mu}\bar{\alpha}_{\lambda\mu}-\alpha_{\lambda\mu}\bar{\alpha}_{\mu\lambda})] , \tag{29}$$

where $V_1 \equiv \cos(k_o R)+(k_o R)\sin(k_o R)$ and $V_2 \equiv (k_o R)^2\cos(k_o R)$. Choosing the photon polarization direction as the Z axis and integrating this result over all the possible orientations of atom B with respect to atom A results in

$$\langle d\Gamma' \rangle = \frac{N_A N_B I |\mu^{mo'}|^2}{108\varepsilon_0^3 \hbar c R^6} \rho_f \alpha_{\lambda\mu} \bar{\alpha}_{\lambda\mu} (6V_1^2 - 4V_1 V_2 + 2V_2^2) . \tag{30}$$

Further integrating the differential transition rate over the spatial distribution of B molecules yields a final pair-absorption rate. Noting that only the R^{-6} term and the $(6V_1^2-4V_1V_2+2V_2^2)$ term have R dependence, the transition rate becomes

$$\Gamma = \int_{R_{\min}}^{R_{\max}} R^2 dR \langle d\Gamma' \rangle$$

$$= \frac{N_A N_B k_o^3 I |\mu^{mo'}|^2 |\alpha_{\lambda\mu}|^2}{108\varepsilon_0^3 \hbar c} \rho_f$$

$$\times \int_{x_{\min}}^{x_{\max}} dx \left\{ \left[\frac{3}{x^4} + \frac{1}{x^2} + 1 \right] + \cos(2x) \left[\frac{3}{x^4} - \frac{5}{x^2} + 1 \right] \right.$$

$$\left. + \sin(2x) \left[\frac{6}{x^3} - \frac{2}{x} \right] \right\} , \tag{31}$$

where $x \equiv k_o R$ and $R_{\min}$ is the minimum equilibrium distance between the atoms A and B, or, in the case of the crystals, $R_{\min}$ can be taken as the lattice constant, and $R_{\max}$ is the bulk size of the gas cell or crystal. Perfecting the integration yields

$$\int_{x_{\min}}^{x_{\max}} dx \{ \cdots \} = \left[-\frac{1}{x^3} - \frac{1}{x} + x - \frac{\cos(2x)}{x^3} - \frac{2\sin(2x)}{x^2} + \frac{\cos(2x)}{x} + \tfrac{1}{2}\sin(2x) \right]_{x_{\min}}^{x_{\max}} . \tag{32}$$

This expression contains several terms, one of which is linearly diverging with the bulk size of the system. This expression predicts that, in the absence of any coherence-destroying processes, the transition probability per unit volume per unit time actually depends on the size of the active volume. This linear term was not found in previous calculations, since all of the previous theories considered only near-field interaction, which depends on the inverse cube of the distance and converges when integrated over the volume. The volume-dependent term appears when the retardation is properly considered, and is important when the separation is larger than the characteristic wavelength. As an estimate of the relative strengths of the various terms for a realistic experimental environment, we take $R_{\min} = 30$ Å, $R_{\min} < R_{\max} < 1$ cm, $\lambda_0 = 5537$ Å. For these typical values, contribution from all terms except $x_{\max}$ and $2/x_{\min}^3$ are negligible.

In practical situations, there exist several decay channels for the excited-state coherence that produce finite linewidths in the interaction. This loss of coherence limits the distance over which a virtual photon from the excited atom can travel before it is dephased as it relaxes to a lower level. This effect can be included in the summation of the differential transition rates over all other atoms by a multiplication factor $\exp(-2\gamma_T R/c)$, where $1/\gamma_T$ is the excited-atom coherence time due to all processes.[34] This is very similar to the case studied by Craig and co-workers for the frequency shift of a guest atom embedded in a crystalline host.[35,36]

Using this approach Eq. (45) can be replaced by

$$\left[-\frac{2}{x^3} + x \right]_{x_{\min}}^{x_{\max}} = \int_{x_{\min}}^{x_{\max}} dx \left[\frac{6}{x^4} + 1 \right] \rightarrow \int_{x_{\min}}^{x_{\max}} dx \left[\frac{6}{x^4} + 1 \right] e^{-\eta x}$$

$$= \left[e^{-\eta x} \left\{ -\frac{2}{x^3} + \frac{\eta}{x^2} - \frac{\eta^2}{x} - \frac{1}{\eta} \right\} - \eta^3 \mathrm{Ei}(-\eta x) \right]_{x_{\min}}^{x_{\max}} , \tag{33}$$

where Ei is the exponential integral function and $\eta \equiv 2\gamma_T / c k_o$. The curve labeled (a) in Fig. 3 shows a plot of Eq. (32) (infinite coherence length) as a function of the active volume size expressed in logarithmic units.

The curves 3(b) and 3(c) are plots of Eq. (33) for the values of $c/2\gamma_T$ (b) 0.5 cm, and (c) 0.1 mm. The inclusion of dephasing mechanisms removes the linear divergence for a sample of infinite size. In systems where the coherence time is limited by purely radiative decay with $\tau \cong 10^{-8}$ sec, however, the coherence length is about a meter, and finite-size effects in the transition rate should be expected. In most crystals, the dephasing time of the active atoms decreases exponentially with temperature. For example, the linewidth in ruby exhibits a rapid exponential increase with temperature, which reduces the dephasing time to a few picoseconds at room temperature.[37] Thus the observation of a sample-size-dependent rate will in general require the use of very low temperatures to increase the coherence of the process.

In the limit that the dephasing time is short, the linear $x_{\max}$ term is negligible compared to the $2/x_{\min}^3$ term, and the main contribution comes from the Coulomb term. Examination of Fig. 3 shows that, except for the $x_{\max}$ term, the contribution to the transition rate is confined to

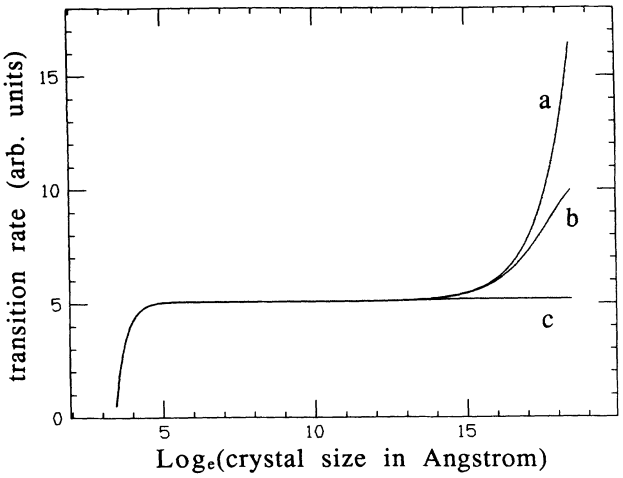

FIG. 3. Crystal-size dependence of the transition probability. Curve (a) is for Eq. (32), which corresponds to the infinite coherence length. The plot of the two dominant terms is indistinguishable from the plot of the full expression [Eq. (32)]. (b) Equation (33) for the coherence length of 0.5 cm; (c) Eq. (33) for the coherence length of 0.1 mm. The parameters used are $R_{\min}=30$ Å, $R_{\min}<R_{\max}<1$ cm, $\lambda_0=5537$ Å.

a narrow region of separations. For example, for $R_{\min}=30$ Å, and $\lambda_0=5537$ Å, the main contribution to the transition rate is due to a region of radius $\cong 100$ Å, and the near-field Coulomb interaction is sufficient to determine the transition rate. In this limit, we have

$$\Gamma=\frac{N_A N_B I|\mu^{mo'}|^2|\alpha_{\lambda\mu}|^2}{54\varepsilon_0^3\hbar c R_{\min}^3}\rho_f \ . \tag{34}$$

In the simplest case of a three-level system, the second term in Eq. (24) can be neglected because of its large denominator, yielding

$$\alpha_{\lambda\mu}\bar{\alpha}_{\lambda\mu}\cong\frac{|\mu^{pr}|^2|\mu^{ro}|^2}{(\hbar\omega-E_{ro})^2} \tag{35}$$

and

$$\Gamma=\frac{N_A N_B I|\mu^{mo'}|^2|\mu^{pr}|^2|\mu^{ro}|^2}{54\varepsilon_0^3\hbar c R_{\min}^3(E_{ro}-\hbar\omega)^2}\rho_f \ . \tag{36}$$

The density of the final states, ρ_f, required to evaluate the transition rate can be calculated in terms of the line-shape functions describing homogeneous pressure broadening in gases and phonon broadenings in crystals. For an exciting laser whose frequency is $\nu_L=\nu_{Lo}+\delta$, where $h\nu_{Lo}=E_{po}+E_{mo'}$, only those pairs of atoms which happen to have detuned energy levels that when added equal ν_L should be available for transitions. This statistical treatment gives a final density of states which is a convolution of the line shapes of atoms A and B:

$$\rho_f\equiv\frac{1}{h}\int_{-\infty}^{\infty}g_A(\nu)g_B(\nu_L-\nu)d\nu \ . \tag{37}$$

In the case where pressure broadening dominates, the single-atomic line shape will be given by the Lorentzian function:

$$g_A(\nu)=\frac{\delta\nu_A/\pi}{(\nu-\nu_p)^2+(\delta\nu_A)^2} \tag{38}$$

and

$$g_B(\nu_L-\nu)=\frac{\delta\nu_B/\pi}{(\nu_L-\nu-\nu_m)^2+(\delta\nu_B)^2}=\frac{\delta\nu_B/\pi}{(\nu-\nu_p-\delta)^2+(\delta\nu_B)^2} \ , \tag{39}$$

where $\delta\nu_A$ is the half width at half maximum. The Lorentzian form for $g(\nu)$ yields an integral expression for the density of final states given by

$$\rho_f\equiv\frac{(\delta\nu_A)(\delta\nu_B)}{\pi^2 h}\int_{-\infty}^{\infty}\frac{dx}{(x^2+\gamma^2)\{(x-\delta)^2+\beta^2\}} \ , \tag{40}$$

where $\nu-\nu_p=x$, $\delta\nu_A=\gamma$, and $\delta\nu_B=\beta$. This integral can be evaluated using contour integration and yields

$$\rho_f=\frac{1}{\pi h}\frac{\delta^2(\beta+\gamma)+(\beta^2-\gamma^2)(\beta-\gamma)}{\delta^4+\beta^4+\gamma^4+2\delta^2\beta^2+2\delta^2\gamma^2-2\beta^2\gamma^2} \ . \tag{41}$$

This density of states function has a peak value at $\delta=0$ given by

$$\rho_f(\delta=0)=\frac{1}{\pi h}\frac{1}{\beta+\gamma} \ .$$

This model predicts a peak density of states which is inversely proportional to the sum of the width of two line shapes. As a special case, if one line shape is very narrow so that we can effectively set $\beta=0$, then

$$\rho_f=\frac{1}{\pi h}\frac{\gamma}{\delta^2+\gamma^2} \ ,$$

which is another Lorentzian function centered at $\nu_{Lo}=\nu_p+\nu_M$. If, on the other hand, the linewidths of the two atoms are the same ($\gamma=\beta$), then the final density of states has the same form as the previous one, except that γ should be replaced by 2γ. From Eq. (36), it is apparent that the transition rate is inversely proportional to the square of the energy difference between the intermediate states of atom A and the exciting laser beam.

In the case where Doppler broadening or phonon broadening dominates in gases and crystals respectively, a Gaussian line shape should be used. Then the line shape is given as

$$g_A(\nu)=\frac{1}{\sqrt{\pi}(\delta\nu_A)}\exp-\left[\frac{\nu-\nu_p}{\delta\nu_A}\right]^2 \tag{42}$$

where $\delta\nu_A=[\text{FWHM}/(4\ln 2)^{1/2}]$, FWHM being the full width at half maximum, and similarly for $g_B(\nu)$. The final density of states according to Eq. (37) is then given by

$$\rho_f=\frac{1}{\sqrt{\pi}h(\gamma^2+\beta^2)^{1/2}}\exp-\frac{\delta^2}{\gamma^2+\beta^2} \ . \tag{43}$$

III. COMPARISON OF THE MODEL TO THE EXPERIMENTAL DATA

In this section we will apply the theory developed to a specific case of pair absorption in solids. The first measurement of pair absorption in a solid was due to Varsanyi and Dieke.[9] Following this work, Dieke and Dorman measured the relative intensities of 90 pair-absorption lines in $PrCl_3$, and found no noticeable polarization dependence.[10] Later, Dorman[27] measured the integrated line intensity for the pair-absorption transition $3H_4+3H_4+25\,397\ \mathrm{cm}^{-1}\rightarrow 3P_0+3F_2(\mu=2)$ and found it to be 1.3×10^{-5} times that of the transition $3H_4+20\,475\ \mathrm{cm}^{-1}\rightarrow 3P_0$. The pair-absorption transition probability integrated over the absorption band, under the assumption that the absorption line profile is Gaussian[27] and has a width much smaller than the detuning, is given by our model as

$$\int \Gamma_{\mathrm{PA}} d\nu = \frac{N^2 I |\mu^{mo'}|^2 |\mu^{pr}|^2 |\mu^{ro}|^2}{432\pi^3 \varepsilon_0^3 \hbar^4 c R_{\min}^3 (\nu_r - \nu_{Lo})^2} , \tag{44}$$

while the one-photon absorption probability integrated over the absorption band is given by

$$\int \Gamma_{\mathrm{OP}} d\nu = \frac{NI|\mu^{po}|^2}{6\varepsilon_0 \hbar^2 c} . \tag{45}$$

The ratio of these integrated transition rates is given by

$$\frac{\int \Gamma_{\mathrm{PA}} d\nu}{\int \Gamma_{\mathrm{OP}} d\nu} = \frac{N|\mu^{mo'}|^2 |\mu^{pr}|^2 |\mu^{ro}|^2}{72\pi^3 \varepsilon_0^2 \hbar^2 R_{\min}^3 (\nu_r - \nu_{Lo})^2 |\mu^{po}|^2} . \tag{46}$$

The unit cell of $PrCl_3$ has a volume of $2.122\times10^{-28}\ \mathrm{m}^3$, and each unit cell contains two praseodymium ions,[38] resulting in a number density of $N=9.427\times10^{27}\ \mathrm{m}^{-3}$, and a nearest-neighbor distance $R_{\min}=4.375$ Å. This small nearest-neighbor distance results in a negligible retardation effect to the pair-absorption rate. For the experiments in Ref. 9, the relevant states are labeled $|o\rangle=|o'\rangle=3H_4$, $|m\rangle=3F_2(\mu=2)$, $|p\rangle=3P_o$, and $|r\rangle=4f5d$. The transition within the $4f^2$ manifold in the gaseous state is forbidden by selection rules, but, in the case of a crystalline environment, the crystal field breaks the inversion symmetry at the ionic site and the transition is allowed.[39] The estimated oscillator strengths[27] for these intrashell transitions are expected to be about 10^{-6}. Because of the strong transition probability, we believe that most likely the intermediate virtual state $|r\rangle$ lies in the $4f5d$ manifold. Unfortunately, spectral lines for these transitions are very broad, and as a consequence the $4f5d$ manifold appears as a broad band. Because of the fact that transitions to the $4f5d$ manifold are in the ultraviolet,[40] not enough data are available to calculate a very reliable value for the matrix element. If in fact the unknown virtual-state energy is the same as the energy of the lower edge of the $4f5d$ band ($61\,170\ \mathrm{cm}^{-1}$), $\nu_{mo}=4922\ \mathrm{cm}^{-1}$, $\nu_{po}=20\,475\ \mathrm{cm}^{-1}$, and the detuning is large, the exact location of the $|r\rangle$ state is not likely to change the order of magnitude of the transition. The oscillator strength[27] of the $3P_0-3H_4$ transition has been measured to be 5.8×10^{-6} for 0.26 at. % Pr:$LaCl_3$; however, the oscillator strength for the $3F_2$-$3H_4$ transition has not been determined, probably because of its very small absorption intensity.

Using the data discussed, the ratio of the pair-absorption rate to the single transition rate in mks units is determined to be

$$\frac{\int \Gamma_{\mathrm{PA}} d\nu}{\int \Gamma_{\mathrm{OP}} d\nu} = 5.0\times10^{112} \frac{|\mu^{mo'2}|\mu^{pr}|^2|\mu^{ro}|^2}{|\mu^{po}|^2} .$$

Assuming that $\mu_{pr}=\mu_{mo'}$, then we expect $\mu_{pr}=\mu_{op}=10^{-30}$ C m for this calculation to be in agreement with the experimental measurement. Furthermore, if we assume that the oscillator strength for the $3F_2$-$3H_4$ transition is smaller than for the transition $3P_o$-$3H_4$ by a factor of 3, then $\mu_{pr}=\mu_{op}=10^{-31}$ C m.[41] Based on this estimate and the sparse data available, the theory gives reasonable agreement with experimental data for stationary ions in solids. More conclusive tests of the rates, and in particular the sample-size dependence predicted, will require more refined measurements for a simpler system where all the parameters are known.

Interestingly, Yen *et al.*[28] have found that the pair absorption in PrF_3 ($3P_0+3F_2$) shows a fairly strong polarization dependence, in contrast to the previously discussed results in Ref. 9. The explanation of such an effect implies that the rotating-atom approximation is not useful in crystalline systems. The case of fixed-ion pair absorption is calculated in what follows and is compared to the results of Yen *et al.*

Assuming that the photon propagation direction is along the Y axis ($\mathbf{k}=k\hat{y}$) and the polarization direction of the linearly polarized incident laser beam is along the Z axis, [$\mathbf{e}_k^{(\lambda)}(\mathbf{k})=\delta_{k,z}$, $\bar{\mathbf{e}}_n^{(\lambda)}(\mathbf{k})=\delta_{n,z}$], Eq. (24) assumes the form

$$d\Gamma = \frac{N_A N_B}{16\pi\hbar\varepsilon_o^3 R^6} \frac{n\hbar c k}{V} \times \mu_i^{mo'} \bar{\mu}_l^{mo'} \alpha_{jz} \bar{\alpha}_{mz} V_{ij}(k_o R) \bar{V}_{lm}(k_o R) \rho_f . \tag{47}$$

Using the same approximation for Eq. (21) as before, we can express the differential pair-absorption rate as

$$d\Gamma = \frac{N_A N_B}{16\pi\hbar\varepsilon_o^3 R^6} \frac{n\hbar c k}{V} \frac{|\mu_z^{ro}|^2}{(\hbar\omega - E_{ro})^2} \times \rho_f \{ |\boldsymbol{\mu}^{mo'}\cdot\boldsymbol{\mu}^{pr}|^2 (V_1 - V_2)^2 + 2(\boldsymbol{\mu}^{mo'}\cdot\boldsymbol{\mu}^{pr})(\bar{\boldsymbol{\mu}}^{mo'}\cdot\hat{R})(\bar{\boldsymbol{\mu}}^{pr}\cdot\hat{R})(V_1 - V_2)(-3V_1 + V_2) + |\boldsymbol{\mu}^{mo'}\cdot\hat{R}|^2 |\boldsymbol{\mu}^{pr}\cdot\hat{R}|^2 (-3V_1 + V_2)^2 \} . \tag{48}$$

As might be expected, for a given pair of atoms, the transition rate is a function of the Z component of the dipole moment of the intermediate transition and of the vector products of the two transition dipole moments with the directional vector. Noting that the orientational dependence is only through the vector products with the dipole vectors, it is convenient to define a new coordinate system for $\hat{R}$ where the $\hat{z}'$ axis is parallel to $\mu^{mo'}$, i.e.,

$$\begin{aligned}
&\mu^{mo'}=|\mu^{mo'}|\hat{z}'=\mu_{z'}^{mo}\hat{z}' ,\\
&\hat{R}=\hat{x}'\sin\vartheta'\cos\phi'+\hat{y}'\sin\vartheta'\sin\phi'+\hat{z}'\cos\vartheta' ,\\
&\mu^{pr}\cdot\hat{R}=\mu_{x'}^{pr}\sin\vartheta'\cos\phi'+\mu_{y'}^{pr}\sin\vartheta'\sin\phi'+\mu_{z'}^{pr}\cos\vartheta' ,
\end{aligned} \tag{49}$$

and

$$(\mu^{mo}\cdot\hat{R})(\bar{\mu}^{pr}\cdot\hat{R})=\mu_{z'}^{mo}\bar{\mu}_{x'}^{pr}\sin\vartheta'\cos\vartheta'\cos\phi'+\mu_{z'}^{mo}\bar{\mu}_{y'}^{pr}\sin\vartheta'\cos\vartheta'\sin\phi'+\mu_{z'}^{mo}\bar{\mu}_{z'}^{pr}\cos^2\vartheta' . \tag{50}$$

Integrating over the orientation of atom B relative to atom A, the differential absorption rate becomes

$$\begin{aligned}
d\Gamma'=&\frac{N_A N_B}{16\pi\hbar\varepsilon_0^3 R^6}\frac{n\hbar ck}{V}\frac{|\mu_z^{ro}|^2}{(\hbar\omega-E_{ro})^2}\\
&\times\rho_f\left[4\pi|\mu^{mo'}\cdot\mu^{pr}|^2(V_1-V_2)^2+\frac{8\pi}{3}(\mu^{mo'}\cdot\mu^{pr})(\bar{\mu}_{z'}^{mo'}\cdot\bar{\mu}_{z'}^{pr})(V_1-V_2)(-3V_1+V_2)\right.\\
&\left.+(-3V_1+V_2)^2|\mu_{z'}^{mo'}|^2\left\{\frac{4\pi}{15}|\mu_{x'}^{pr}|^2+\frac{4\pi}{15}|\mu_{y'}^{pr}|^2+\frac{4\pi}{5}|\mu_{z'}^{pr}|^2\right\}\right] .
\end{aligned} \tag{51}$$

Remembering that $\bar{\mu}_{z'}^{mo'}\cdot\bar{\mu}_{z'}^{pr}=\bar{\mu}^{mo'}\cdot\bar{\mu}^{pr}$ and $|\mu_{z'}^{mo'}|^2=|\mu^{mo'}|^2$, the quantity inside the outermost square bracket is given by

$$[\cdots]=\frac{4\pi}{15}|\mu^{mo'}\cdot\mu^{pr}|^2(3V_1^2-2V_1V_2+7V_2^2)+\frac{4\pi}{15}|\mu^{mo'}|^2|\mu^{pr}|^2(9V_1^2-6V_1V_2+V_2^2) . \tag{52}$$

Using similar steps as in Eqs. (27)–(32), the overall pair-transition rate is found to be

$$\begin{aligned}
\Gamma=&\frac{N_A N_B k^3}{120\pi\hbar\varepsilon_0^3}\frac{n\hbar ck}{V}\frac{|\mu_z^{ro}|^2}{(\hbar\omega-E_{ro})^2}\rho_f\\
&\times\left[|\mu^{mo'}|^2|\mu^{pr}|^2\left\{\left[\frac{1}{2}-\frac{6}{x^2}\right]\sin 2x+\left[\frac{3}{x}-\frac{3}{x^3}\right]\cos 2x-\frac{3}{x^3}-\frac{3}{x}+x\right\}\right.\\
&\left.+|\mu^{mo'}\cdot\mu^{pr}|^2\left\{\left[\frac{7}{2}-\frac{2}{x^2}\right]\sin 2x+\left[\frac{1}{x}-\frac{1}{x^3}\right]\cos 2x-\frac{1}{x^3}-\frac{1}{x}+7x\right\}\right]_{x_{\min}}^{x_{\max}} .
\end{aligned} \tag{53}$$

Retaining only the dominant terms in the presence of a dephasing mechanism, we have

$$\Gamma=\frac{N_A N_B I}{60\hbar c\varepsilon_0^3 R_{\min}^3}\frac{|\mu_z^{ro}|^2\{3|\mu^{mo'}|^2|\mu^{pr}|^2+|\mu^{mo'}\cdot\mu^{pr}|^2\}}{(\hbar\omega-E_{ro})^2}\rho_f . \tag{54}$$

The result is slightly different from the case of the rotating-atom approach. This expression ($\Gamma\propto|\mu_z|^2\propto\cos^2\vartheta=1-\sin^2\vartheta$) should be compared to the experimentally determined polarization dependence ($\Gamma\propto 1-0.45\sin^2\vartheta$) found by Yen *et al.*[28] Clearly these two dependences are different. However, the model employed has assumed no crystalline-symmetry dependence or matrix-element orientations. Although numerous experiments have been done on gas mixtures, this polarization dependence has not been found, due to the fact that atomic dipoles can point in any direction and are averaged in the contribution to the transition probability. In the crystal case, the C axis provides a unique axis for the dipole moment. Further experiments will shed light on this dependence and will again provide more of the required data to include crystalline anisotropy into the fixed-ion theory presented.

ACKNOWLEDGMENTS

The authors are indebted to the U.S. Air Force Office of Scientific Research for support of the work. The authors are also grateful to Professor Anderson Gomes for many helpful suggestions.

[1]M. F. Crawford and H. L. Welsh, Phys. Rev. **75**, 1607 (1949).
[2]R. Coulon, L. Galatry, J. Robin, and B. Vodar, Discuss. Faraday Soc. **22**, 22 (1936).
[3]J. Fahrenfort and J. A. A. Ketelaar, J. Chem. Phys. **22**, 1631 (1954).
[4]J. A. A. Ketelaar, Rec. Trav. Chim. **75**, 857 (1956).
[5]J. P. Colpa and J. A. A. Ketelaar, Mol. Phys. **1**, 14 (1958).
[6]J. A. A. Ketelaar and F. N. Hooge, J. Chem. Phys. **23**, 749 (1955).
[7]J. A. A. Ketelaar and F. N Hooge, Rec. Trav. Chim. **76**, 529 (1957).
[8]H. P. Gush, W. F. J. Hare, E. J. Allin, and H. L. Welsh, Can. J. Phys. **38**, 176 (1960).
[9]F. Varsanyi and G. H. Dieke, Phys. Rev. Lett. **7**, 442 (1961).
[10]G. H. Dieke and E. Dorman, Phys. Rev. Lett. **11**, 17 (1963).
[11]E. Nakazawa and S. Shionoya, Phys. Rev. Lett. **25**, 1710 (1970).
[12]J. P. Colpa and J. A. A. Ketelaar, Physica **24**, 1035 (1958).
[13]Toru Miyakawa and D. L. Dexter, Phys. Rev. B **1**, 70 (1970).
[14]J. R. Rios Leite and Cid B. De Araujo, Chem. Phys. Lett. **73**, 71 (1980).
[15]D. L. Dexter, Phys. Rev. **126**, 1962 (1962).
[16]J. Van Kranendonk, Can. J. Phys. **38**, 240 (1960).
[17]J. D. Poll and J. Van Kranendonk, Can. J. Phys. **39**, 189 (1961).
[18]J. P. Colpa, in *Physics of High Pressures and the Condensed Phase,* edited by A. Van Itterbeek (North-Holland, Amsterdam, 1965), Chap. 12.
[19]L. I. Gudzenko and S. I. Yakovlenko, Zh. Eksp. Teor. Fiz. **62**, 1686 (1972) [Sov. Phys. JETP **35**, 877 (1972)].
[20]L. I. Goodzenko and S. I. Yakovlenko, Phys. Lett. A **46**, 475 (1974).
[21]J. C. White, G. A. Zdasiuk, J. F. Young, and S. E. Harris, Opt. Lett. **4**, 137 (1979).
[22]J. C. White, G. A. Zdasiuk, J. F. Young, and S. E. Harris, Phys. Rev. Lett. **41**, 1709 (1978).
[23]R. Hotop and K. Niemax, J. Phys. B **13**, L93 (1980).
[24]J. C. White, Phys. Rev. A **23**, 1698 (1981).
[25]J. C. White, Opt. Lett. **6**, 242 (1981).
[26]F. Roussel, Comments At. Mol. Phys. **15**, 59 (1984).
[27]E. Dorman, J. Chem. Phys. **44**, 2910 (1966).
[28]W. M. Yen, C. G. Levey, Shihua Huang, and Shui T. Lai, J. Lumin. **24/25**, 659 (1981).
[29]Eiichiro Nakazawa and Shigeo Shionoya, Phys. Rev. Lett. **25**, 1710 (1970).
[30]A. S. L. Gomes, G. S. Maciel, R. E. de Araújo, L. H. Acioli, and Cid B. de Araújo, Opt. Commun. (to be published).
[31]*Spectroscopy of Solids Containing Rare Earth Ions. Modern Problems in Condensed Matter Sciences,* edited by A. A. Kaplyanskii and R. M. Macfarlane (North-Holland, Amsterdam, 1987), Vol. 27.
[32]S. E. Harris and J. C. White, IEEE J. Quantum Electron. **13**, 972 (1977).
[33]D. P. Craig and T. Thirunamachandran, *Molecular Quantum Electrodynamics* (Academic, London, 1984), p. 208.
[34]M. J. Stephen, J. Chem. Phys. **40**, 669 (1964).
[35]D. P. Craig and P. D. Dacre, Proc. R. Soc. London, Ser. A **310**, 297 (1969).
[36]D. P. Craig and L. A. Dissado, Proc. R. Soc. London, Ser. A **310**, 313 (1969).
[37]A. Yariv, *Quantum Electronics,* 3rd ed. (Wiley, New York, 1989), p. 205.
[38]K. Shinagawa, J. Phys. Soc. Jpn. **23**, 1057 (1967).
[39]E. V. Sayre, K. M. Sancier, and S. Freed, J. Chem. Phys. **23**, 2060 (1955).
[40]L. R. Elias, Wm. S. Heaps, and W. M. Yen, Phys. Rev. B **8**, 4989 (1973).
[41]A. G. Svetashev and M. P. Tsvirko, Opt. Spektrosk. **51**, 1034 (1981) [Opt. Spectrosc. **51**, 572 (1981)].

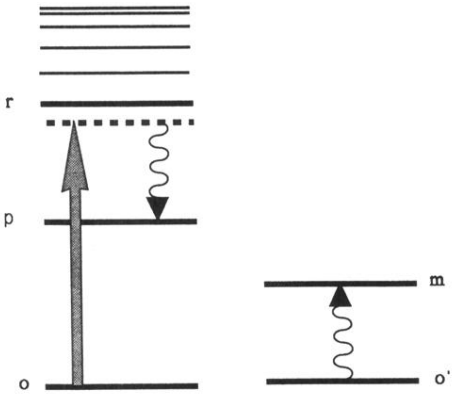

FIG. 1. Relevant energy levels for the pair-excitation process.